Pulsed Terahertz Signal Reconstruction

J. R. Fletcher, G. P. Swift,[a] DeChang Dai, and J. M. Chamberlain
Department of Physics, University of Durham, Durham DH1 3LE, United Kingdom

P. C. Upadhya
School of Electronic and Electrical Engineering, Leeds University, Leeds LS2 9JT, United Kingdom

(Received 26 June 2007; accepted 5 October 2007; published online 6 December 2007)

A procedure is outlined which can be used to determine the response of an experimental sample to a single, simple broadband frequency pulse in terahertz frequency time domain spectroscopy (TDS). The advantage that accrues from this approach is that oscillations and spurious signals (arising from a variety of sources in the TDS system or from ambient water vapor) can be suppressed. In consequence, small signals (arising from the interaction of the radiation with the sample) can be more readily observed in the presence of noise. Procedures for choosing key parameters and methods for eliminating further artifacts are described. In particular, the use of input functions which are based on the binomial distribution is described. These binomial functions are used to unscramble the sample response to a simple pulse: they have sufficient flexibility to allow for variations in the spectra of different terahertz sources, some of which have low frequency as well as high frequency cutoffs. The signal processing procedure is validated by simple reflection and transmission experiments using a gap between polytetrafluoroethylene (PTFE) plates to mimic a void within a larger material. It is shown that a resolution of 100 μm is easily achievable in reflection geometry after signal processing. © *2007 American Institute of Physics*. [DOI: 10.1063/1.2818361]

I. INTRODUCTION

Pulsed terahertz frequency broadband systems are now widely used to investigate the optical properties of a diverse range of materials, including materials of biomedical interest,[1] over a wide spectral range. In such a pulsed terahertz system, a laser triggered source[2] is used and there is little control over the time dependence of the output pulse. For a photoconductive source, the initial pulse of electric field radiated by the carrier acceleration is followed by a collection of after-runners generated by several processes, many of which are unavoidable. Echoes resulting from reflections in the source structure produce delayed and dispersed repeats of the initial output. Propagation through the atmosphere results in absorption at the resonant frequencies of water molecules. Subsidiary oscillations within the source can add further after-runners. Moreover, these are not independent effects. For example, source echoes also excite water vapor oscillations, and echoes can arise in other places, notably in the detector. If the terahertz pulse is transmitted through a dispersive region, such as a waveguide, the various frequency components suffer varying phase changes and delays, further compounding the complexity of the signal. The result is that the signal finally detected has a more complicated form than would be expected from the carrier motion alone.

For measurements of the frequency dependent transmission of a specimen, these after-runners are not disabling, as the main criterion is the frequency content of the incident and transmitted signals. However, for a system using time delay measurements, it would be desirable to have a single simple source pulse. The signal returned by the sample under observation may contain components with several different delays. This will cause confusion between echoes in the source output and overlapping pulses from the sample. If the returned signal includes both weak and strong echoes, the weak signals may be obscured by the source after-runners.

The pulse reconstruction algorithm described in this paper addresses these problems by numerically processing the sample signal together with a reference signal, which has been separately recorded, to remove the undesired effects of the source after-runners. The result is to show what the sample signal would be if the sample had received a single, simple pulse of a form that can be chosen appropriately. The reference signal is produced in such a way that it includes all the distorting effects, but without the influence of the sample. For example, in a reflection measurement the reference signal could be obtained by replacing the sample with a mirror.

II. PRINCIPLE OF PULSE RECONSTRUCTION

At the power levels available from pulsed terahertz sources, the response of the sample is linearly proportional to the input field. The signal, $s(t)$, emerging from the sample can be written as a convolution of the electric field of the source pulse, $f(t)$, arriving at the sample with the impulse response function, $g(t)$, for the sample,

$$s(t) = g(t) \otimes f(t). \tag{1}$$

The response function, $g(t)$, for a unit impulse at $t=0$ is in general a sum (or integral) of delayed impulses at times $t_p(\geqslant 0)$ with amplitudes A_p,

$$g(t) = \sum_p A_p \delta(t - t_p). \tag{2}$$

The signal from the sample then has the form

[a]Electronic mail: g.p.swift@durham.ac.uk

$$s(t) = \sum_p A_p f(t - t_p). \tag{3}$$

A transformation of the source pulse f can be calculated by taking a convolution of a transformation generating function, $u(t)$, with f. The new reconstructed input pulse is then

$$\tilde{f}(t) = u(t) \otimes f(t). \tag{4}$$

Applying the same transformation to the sample signal produces the reconstructed signal,

$$\tilde{s}(t) = u(t) \otimes s(t) = \sum_p A_p \tilde{f}(t - t_p). \tag{5}$$

Comparing Eqs. (3) and (5) shows that the reconstructed signal $\tilde{s}$ is the response the sample would produce to the input signal $\tilde{f}$. The transformation generating function u can be chosen in many ways, but should result in a new input $\tilde{f}$, satisfying several conditions, which are now discussed.

A. Choice of input pulse $\tilde{f}(t)$

In order to make clear the observation of time separated return signals from the sample, the reconstructed input signal should be well localized in time, with no significant fore-runners or after-runners. The length of the input should be short enough to resolve the time intervals between sample echoes, but not so short that its frequency spectrum extends much beyond the range of the terahertz source. Shorter input signals result in increasing noise in the reconstructed sample signal. The choice of the input signal and corresponding transformation u is therefore a compromise between time resolution and noise filtering. This compromise is optimized by choosing an input $\tilde{f}$ that has a frequency spectrum with zero content beyond a chosen cutoff frequency. This eliminates higher frequency noise components. At the same time, the subsidiary fore-runners and after-runners should be as small as possible to avoid hiding a weak signal in the vicinity of a strong one. The corresponding problems of the apodization of diffraction effects, antenna side lobes, and the design of rf channel filters have been discussed in the literature[3] and a wide variety of solutions described.

In this paper, we propose a set of input functions based on the binomial distribution. These have sufficient flexibility to allow for variations in the spectra of different terahertz sources, some of which have low frequency as well as high frequency cutoffs.

B. Binomial forms

The amplitudes of the subsidiary forerunner and after-runner of the input pulse, $\tilde{f}(t)$, are related to the behavior of the spectrum of $\tilde{f}$ as it approaches the cutoff frequency f_c. If the spectrum goes discontinuously to zero, it will result in relatively large subsidiaries to $\tilde{f}$, with amplitudes diminishing slowly away from the main part of the pulse. It is therefore preferable to design $\tilde{f}$ in such a way that its spectrum and the first few derivatives of the spectrum go smoothly to zero at the chosen cutoff frequency. This corresponds to an input pulse that has only a few small subsidiaries close to the main part of the pulse. The frequency spectrum of $\tilde{f}$ is taken as

$$\tilde{F}(\omega) = e^{i\omega t_0}\left[\cos\left(\frac{\omega}{4f_c}\right)\right]^p\left[i\sin\left(\frac{\omega}{2f_c}\right)\right]^q \quad |\omega| \leqslant 2\pi f_c, \tag{6a}$$

and

$$\tilde{F}(\omega) = 0 \quad |\omega| > 2\pi f_c, \tag{6b}$$

where t_0 is the time of arrival of the main part of the source pulse, and the cutoff frequency f_c should not be taken beyond the effective range of the source. The arguments of the trigonometric factors are chosen so that the frequency spectrum is continuous at the cutoff frequency.

The non-negative integers p and q are chosen to suit the requirements of a particular source spectrum, with $(p+q) > 0$. For most sources, p can be taken to be a small integer with $q=0$. This results in an input pulse $\tilde{f}$ with a single maximum and width $\sim f_c^{-1}$. For sources deficient in power at low frequency, better noise reduction is achieved by increasing q to a small integer. This results in an input pulse with $(q+1)$ half-cycles. For observation of a weak pulse in the close vicinity of a strong pulse, the subsidiary oscillation of $\tilde{f}$ must be strongly attenuated. Larger values of $(p+q)$ will produce this attenuation. The parameters $p=2$ and $q=0$ correspond to the van Hann filter.[3]

Numerically, the spectrum $\tilde{F}$ can be taken from Eqs. (6a) and (6b) or more conveniently generated by using the fast Fourier Transform of a simple "seed" function. The seed is generated by convolving together p identical factors of type A with q identical factors of type B, where

$$A = \left[\delta(t) + \delta\left(t - \frac{1}{2f_c}\right)\right] \Big/ 2, \tag{7a}$$

$$B = \left[\delta(t) - \delta\left(t - \frac{1}{f_c}\right)\right] \Big/ 2. \tag{7b}$$

The seed is a collection of δ functions with amplitudes equal to binomial coefficients and oscillating signs when $q>0$. The binomial coefficients arise from expanding the powers of the trigonometric factors expressed in the complex exponential form. The same coefficients occur in the repeated convolutions of functions A and B. Cutting off the spectrum of the seed at $\pm f_c$ and inverting the Fourier Transform gives the form of the input pulse $\tilde{f}$. Figure 1 shows an example of seed and pulse forms.

III. RECONVOLUTION OF THE FILTERED SIGNAL

The relationship between the source pulse, $f(t)$, and the required transformation, $u(t)$, is given by Eq. (4). In frequency space, this gives

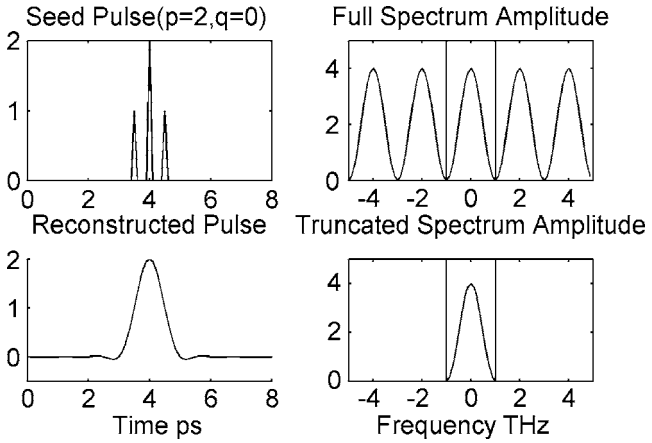

FIG. 1. Seed pulse and reconstructed source pulse.

$$U(\omega) = \frac{\tilde{F}(\omega)}{F(\omega)}. \tag{8}$$

The spectrum of the reconstructed sample pulse, $s(t)$, then follows from Eq. (5),

$$\tilde{S}(\omega) = S(\omega)\frac{\tilde{F}(\omega)}{F(\omega)}, \tag{9}$$

where the upper case symbols indicate Fourier transforms.

The reconstructed output pulse is given by the inverse Fourier transform of $\tilde{S}$. The frequency cutoff in the construction of $\tilde{F}$ avoids the artifacts that would arise from dividing by random noise values beyond the range of the source. This process can be regarded as a "reconvolution," the original convolution of the response function with input f [Eq. (1)] being replaced by convolution with a chosen new input $\tilde{f}$.[4]

IV. ELIMINATION OF ARTIFACTS IN THE RECONSTRUCTION

A. Signal truncation

Spurious effects can appear in the reconstruction if the length of the time scan is insufficient to record the full range of source and sample signals. For example, if the sample produces a large delay, an echo in the source signal may be missed in recording the sample signal.

The fast Fourier transform routines used in processing the signals have the implicit assumption of periodicity beyond the recorded range. The effects of signal truncation then appear as spurious signals which can precede the incident pulse. These artifacts can be removed by the application of an exponential convergence factor. If the recorded source (or reference) signal and sample signal are multiplied by a decreasing exponential, $\exp(-bt)$ and the reconstructed signal multiplied by an increasing exponential $\exp(bt)$, the effects of this truncation can be minimized. Parameter b is chosen so that the recorded signals are reduced smoothly toward zero at the end of the time scan.

B. Water vapor absorption

Water vapor in the atmosphere has several sharp absorptions at frequencies in the terahertz range. Both the source and sample signals can be reduced to noise at these frequencies. Equation (9) shows that the reconstruction will contain narrow bandwidth noise at the water vapor resonances, but other frequencies will not be affected. The spectrum of the reconstructed pulse will have isolated noise peaks at the water vapor resonances, with lower noise over the remainder of the frequency range. This type of noise can be eliminated by applying a filter.

After removing the phase factor, $\exp(i\omega t_0)$, from the Fourier transform of the reconstructed sample pulse, the rapid oscillations of the real and imaginary parts are reduced, except at the water vapor resonances where there may be anomalously large positive or negative values. The effect of these noise peaks can be removed from the reconstruction by replacing $a(n)$ by $\frac{1}{2}[a(n+1)+a(n-1)]$ when

$$[a(n) - a(n-1)][(a(n) - a(n+1)\ ] > C, \tag{10}$$

where $a(n)$ is the nth component of the real or imaginary parts of the Fourier transform, and cutoff level C is chosen so that only the anomalous values are altered and the remaining values are unchanged. After filtering, the phase factor is replaced. This form of filter does not reduce the information content of the reconstructed signal.

C. Choice of parameters

This method of pulse reconstruction is sufficiently flexible to be adapted to a wide range of applications. The optimum choice of the parameters to be used can best be decided by inspection of the reconstructed pulse and its spectrum.

The parameter p with value of 2 is suitable for most types of signal, as this gives amplitudes of the subsidiary oscillations of the source less than 3% of the main peak. If it is necessary to detect a weak signal in the vicinity of a strong pulse, larger values of p will reduce the fore-runners and after-runners of the strong pulse.

The interpretation of the reconstructed signal is most transparent when $q=0$. This gives a single positive peak to the incident pulse, and relative signs of the pulses from the sample are immediately apparent. However, if the source is deficient in low frequency power, taking $q=0$ may result in the appearance of excessive noise at the low frequency end of the spectrum of the reconstructed signal. Larger values of q give incident source pulses with $(q+1)$ half-cycles of alternating signs. Such pulses have reduced low frequencies and result in less low frequency noise, but can cause confusion in the interpretation of close or overlapping sample pulses. Low frequency noise can also be reduced by applying a high pass filter to the reconstruction.

The cutoff frequency f_c controls the time resolution limit $\sim 1/f_c$. This must be related to the maximum frequency of response of the terahertz source and detector. If f_c is chosen too high, $F(\omega)$ in Eq. (9) will have small random values within the range where $\tilde{F}(\omega)$ is nonzero. This will result in strong high frequency noise in the reconstruction. Choosing small values of f_c gives good noise reduction at the expense

of time resolution. The need for a convergence factor will be apparent if the reconstruction produces a spurious precursor before the main sample pulse. This arises when the length of the time scan is insufficient to record the full length of the signal. If the length of scan cannot be conveniently increased, the reconstruction can be improved by the use of a convergence factor, as above, with parameter b having a value of a small multiple of the inverse time scan length.

The cutoff level C for removing the effects of water vapor can be selected by averaging the left side of Eq. (10) over the length of the data and operating the cutoff when the local value exceeds the average by a chosen factor [e.g., 15]. The results of this filtering can be assessed by examination of the spectrum of the reconstructed signal. If the spectrum has a single large anomaly and several smaller anomalous values, a first application of the filter will only remove the largest anomaly. A second application will then remove the remaining smaller anomalies. The results of this filtering are shown in Fig. 3(b).

V. VALIDATION

To validate this approach, two types of experimental measurements were made. In each case, a "phantom" was used which mimics, in a simple way, a void (defect) or "impurity" concealed within another material. In the first set of measurements, the transmission through one or two parallel slabs of material was measured. In the second set, reflection measurements from two parallel slabs of a material were performed. As is well known, pulse reflections will take place at various interfaces within the sample (accompanied, in some cases, by a phase reversal of the signal). By measuring the time position of such peaks, it is, of course, possible to determine the location and separation of particular surfaces. Of course, as the gap is reduced the reflected pulses begin to overlap and merge together, thus getting lost in the background structure of the incident pulse. The two sets of measurements presented here show that the use of the post-detection software routines can "clean up" the signals significantly, and it is possible to determine the size of a much smaller separation than could be obtained from the unprocessed measurement. In reality, this gap might be a defect or an actual buried object located within the medium.

A. Transmission through slabs

Terahertz transmission was investigated through two slabs of various materials, with a varying gap between them, using a standard terahertz transmission setup previously described.[5] The first, stationary, slab was placed with its back surface (furthest from the emitter) at the terahertz beam focus, of spot size approximately 2 mm, while the second slab was placed nearer to the receiver on a translation stage, allowing the gap between the slabs to be varied from 5 mm to 10 μm. Materials investigated were two identical pieces of card, with thickness of 340 μm and terahertz frequency refractive index of 1.36, two identical slabs of polytetrafluoroethylene (PTFE) sheet, with refractive index of 1.42 and thickness of 1.55 mm. The two signals used in the reconstruction are the terahertz signal transmitted through the sample, with the reference signal being that measured without a sample in the system.

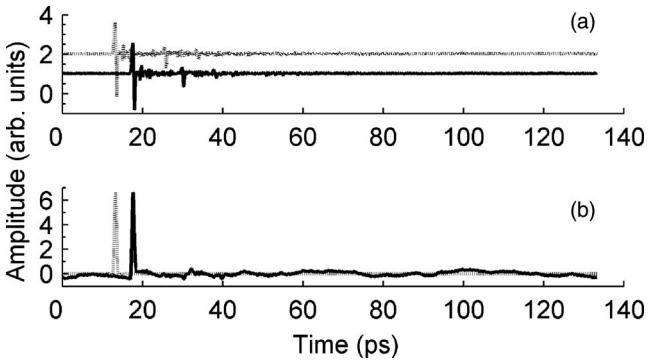

FIG. 2. Reference signal (dotted) and signal transmitted through two slabs of PTFE with 1 mm gap (solid) (a). Reconstructed pulses (b).

Figure 2(a) shows the incident (dotted) and transmitted (solid) signals on two PTFE slabs with a 1 mm gap between them. The signals are essentially the same, with the transmitted signal being a delayed version of the transmitted one. Both signals are strongly affected by atmospheric water vapor absorption and contain echoes from both the source and detector so that internal reflections within the slabs cannot be seen. A simple calculation, using the Fresnel equations, indicates that these reflections are of the order of a few percent of the directly transmitted amplitude. The reconstruction of these signals can be seen in Fig. 2(b), with parameters $p=2$ and $q=0$. In this case, the transmitted signal (solid) represents the response of the system to the simple, single input signal (dotted). Clearly, this input signal has been "cleaned" of both water vapor absorptions and system echoes, while the structure evident in the reconstructed sample signal at longer times is due to internal reflections and absorption processes within the sample. PTFE has no appreciable dispersion over this frequency range, and the phase changes introduced by the sample correspond to simple time delays.

An enlargement of the first 60 ps of the reconstructed signals is shown in Fig. 3(a); as before the reference signal is dotted, while the transmitted signal is solid. The dashed

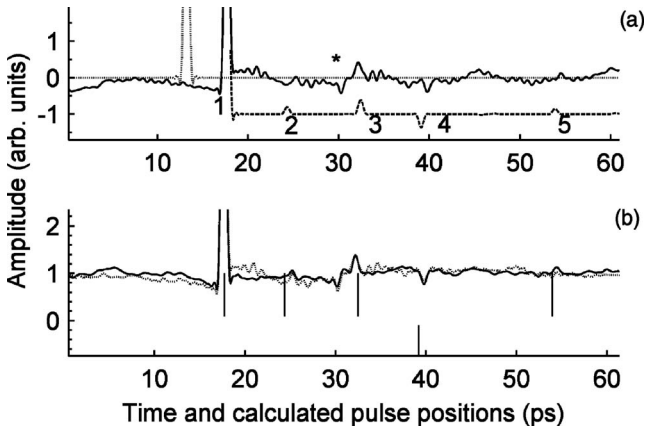

FIG. 3. Reference pulse (dotted), transmitted pulse (solid), and simulated pulse (dashed) through two slabs of PTFE with 1 mm gap (a). The transmitted pulse from (a) after further processing: Nonpurged (dotted) and purged (solid) (b).

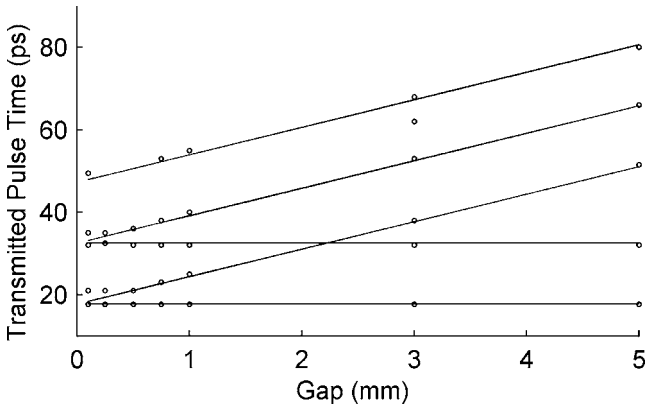

FIG. 4. Delay vs gap for PTFE slabs (transmission).

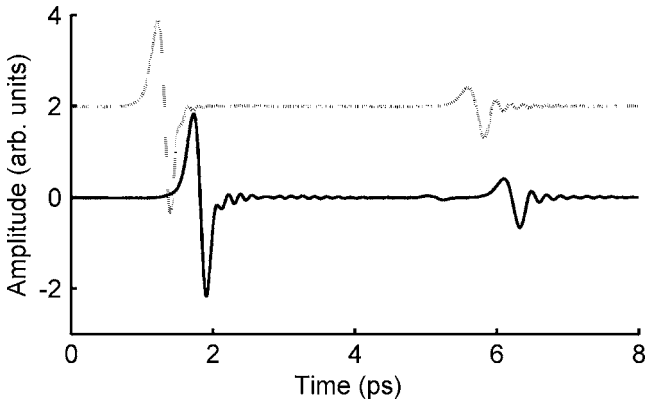

FIG. 5. Transmission through one sheet of PTFE, source (dotted) and sample (solid).

pulse (offset for clarity) represents a theoretical simulation of the response of the system to the seed pulse calculated via a transfer matrix method, using the parameters stated above; the peaks in this signal correspond to internal reflections at the system interfaces. Thus the peak (1) after 17.7 ps is the directly transmitted pulse; (2) after 24.4 ps is the pulse which passes through the first slab, is reflected twice in the air gap, and then passes through the second slab; (3) at 32.5 ps is the pulse which is reflected twice inside one of the slabs, but passes directly through the other; (4) with delay 39.2 ps is the pulse which passes through the first slab, is reflected from the front surface of the second slab, and then the front surface of the first slab; and (5) after 54.0 ps passes through the first slab, is reflected from the back surface of the second slab, off the front of the first slab, and finally is detected. The phase reversed signal, peak (4) is due to there being an odd number of reflections from air to slab (low to high refractive index) boundaries. It should also be noted that the amplitudes of the reconstructed peaks are in agreement with the predictions of the Fresnel equations. The small reconstructed peak after 30.2 ps, marked (*), is of unknown origin, but is probably due to leakage of a system echo through the reconstruction algorithm.

It is clear that internal reflection delays found using the reconstruction process are in good agreement with the calculated peak times. The slight discrepancies, more noticeable at later times, are due to the focused nature of the beam; after multiple reflections the beam has begun to diverge, decreasing the collection efficiency of the setup, thus smearing out the pulses. Without the cleaning up procedure used here in the postdetection processing these multiple transitions would not be observed, and thus the presence of a gap in the sample not determined. Further filtering of this data is shown in the dotted curve of Fig. 3(b); the filter removes outlier points from the experimental data which have evident noise characteristics. The solid curve in Fig. 3(b) is the identical reconstruction carried out in a purged nitrogen atmosphere, with the bars representing the calculated pulse times. Clearly, using a purged system has no real advantages over conducting the experiments in a nonpurged atmosphere if the signal processing routine is applied.

Figure 4 shows the experimentally determined delays, compared with the calculated values for a range of separations for the two sheets of PTFE. The two curves running parallel to the x axis represent the directly transmitted pulse and a pulse reflected in one slab, while the other lines are for those reflected in the varying air gap and zero, one, and two slabs, respectively. A resolution of 500 μm is easily seen in this setup. Similar results (not shown) were seen for transmission of terahertz pulses through thin sheets of card.

Terahertz transmission through a single layer of PTFE was also measured in a dry atmosphere in a system with responses up to ~7 THz.[6] The source signal (dotted), shown in Fig. 5, contained echoes and after-runners, which also appear in the transmitted signal (solid). After reconstruction of the signals to remove the source echo at 6–7 ps, a strongly attenuated pulse could be seen at ~5.2 ps caused by two reflections at the back and front faces of the sample (see Fig. 6). The experiment thus yields the delay of the directly transmitted pulse and the extra delay after two internal reflections. This is sufficient to determine independently both the thickness and the refractive index of the sample. For measured delays of 0.5 and 3.7 ps, respectively; this gives a refractive index value of 1.45 for a sample thickness of 0.33 mm.

B. Reflection by slabs

The terahertz frequency reflections reported here were carried out using a modified terahertz frequency time domain

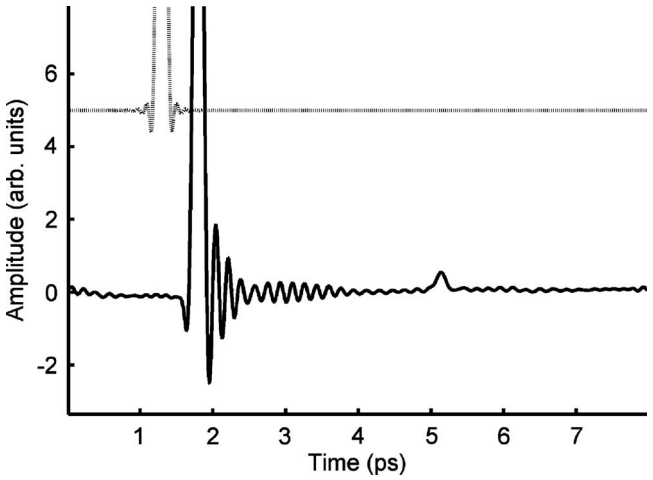

FIG. 6. Reconstruction of terahertz pulse on transmission through one sheet of PTFE, source (dotted) and sample (solid).

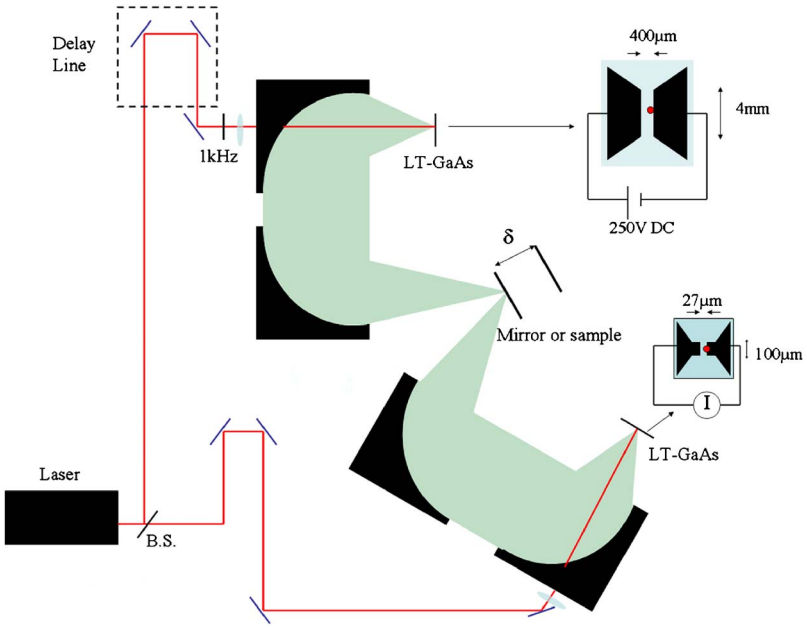

FIG. 7. (Color online) Terahertz reflection experimental arrangement.

spectroscopy (TDS) arrangement, shown schematically in Fig. 7. After generation of the terahertz frequency radiation, using the same method as the transmission setup, the radiation was collected using reflection geometry[7] and collimated using a parabolic mirror with focal length of 5 cm, before being focused onto the reflection point, angled at 27° to the normal using a 15 cm focal length mirror, with effective spot size of 3 mm. The reflected radiation was then collected by another mirror with focal length of 15 cm, before being focused onto the photoconductive detector using a parabolic mirror with focal length of 7.5 cm. The terahertz beam on the detector is superimposed on the probe laser beam, which is formed by splitting 30% from the pump beam. All parabolic mirrors used had diameter of 5 cm. The receiver was again fabricated on "low temperature grown" GaAs,[8] this time using bow tie electrodes with length of 100 μm and width of 27 μm. The current induced by the terahertz radiation was initially preamplified before detection using lock-in techniques, referenced to a 1 kHz mechanical chopper placed in the pump arm, so that the electric field of the terahertz pulse could be measured. Terahertz pulses with signal to noise ratio of approximately 1200:1 were routinely obtained using this system, which could be enclosed in a dry box to allow measurements to be made in a purged nitrogen atmosphere if required. The reference signal for these measurements was obtained by replacing the sample with a mirror. To investigate the minimum resolution of a gap between the slabs of PTFE and cardboard from above, the second slab was placed on a translation stage behind the slab, once again allowing gap sizes from 5 mm to 10 μm to be investigated.

Figure 8(a) shows the incident (dotted) and reflected (solid) signals on two PTFE slabs with a 1 mm gap between them. In this scenario, the signals are very different from one another: the larger amplitude signal seen at 21.8 ps in the reference scan is due to reflections of unknown origin within the semiconductor emitter and receiver; the smaller signal at 34.2 ps is a secondary echo. The reflected signal from the sample is much weaker than the reference signal; this is approximately 15% of the reference amplitude, in good agreement with the Fresnel equations. Once again, both signals are affected by atmospheric water vapor absorption, but less so than when electro-optic crystal detection is used. Figure 8(b) is an enlargement of the signal reflected from the PTFE; again, system echoes are clearly evident in this signal as are a number of phase reversed pulses. Reflections from the front surface of the PTFE are of the same phase as the reference signal, both having low to high refractive index, while back surface reflections have a relative phase reversal. It may be possible to identify the surfaces responsible for these reflected signals, but without prior knowledge of the slab properties completely certain identification is not possible.

The reconstruction of these signals can be seen in Fig. 9(a), with parameters $p=2$ and $q=0$; addition of a high pass filter, as opposed to taking $q>0$, was found to be more useful in removing low frequency noise. Clearly, the dotted input signal has been "cleaned" of both water vapor absorptions and, especially, the system echoes, while the structure evident in the reconstructed sample signal (solid) at longer times is due to reflections from the slab boundaries and ab-

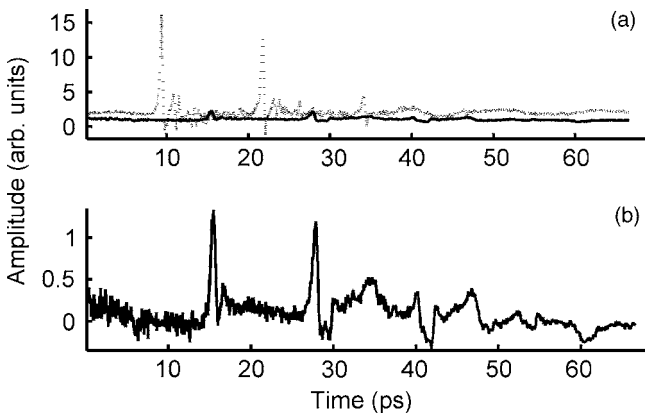

FIG. 8. Reference signal (dotted) and signal reflected from two pieces of PTFE 1 mm apart (solid) (a). Enlarged reflected signal (b).

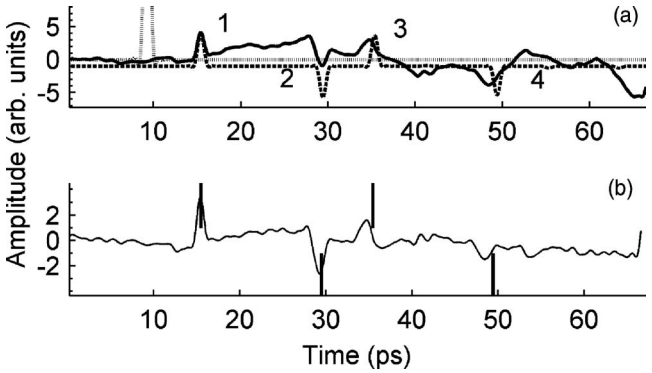

FIG. 9. Reference pulse (dotted), reconstructed reflected pulse (solid), and simulated pulse (dashed) for 1 mm gap (a). Further processed reflected signal (b).

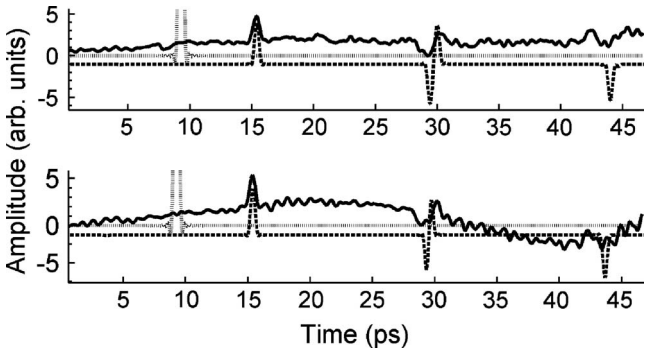

FIG. 11. Reference pulse (dotted), reconstructed reflected pulse (solid), and simulated pulse (dashed) for 100 μm gap (a). Reference pulse (dotted), reconstructed reflected pulse (solid), and simulated pulse (dashed) for 40 μm gap (b).

sorption processes within the sample. The dashed line represents a theoretical simulation of the response of the system to the seed pulse calculated via a transfer matrix method using the parameters stated above. Peak (1) at 15.4 ps is the reflection from the surface of the first sheet of PTFE: this is delayed from the reference signal because the surface of this is not quite at the same point in space as the reflecting mirror, so a path length increase has been introduced. Line (2), phase reversed, after 29.4 ps is the reflection from the back surface of the first sheet. Line (3) 35.3 ps is the reflection from the front of the second sheet. Line (4) 49.4 ps is the reflection from the back surface of the second sheet. Application of the smoothing filter to the reconstructed reflected signal is shown in Fig. 9(b), with the bars representing the calculated reflection times. In this case, it is found that further filtering is not helpful, since the source spectrum does not go to zero at the water vapor resonances. The mathematical reconstruction, however, has cleaned up the reflected signals, removing the very large system echo and allowing proper identification of the surface positions of various layers.

Reconstruction of the reflected pulses seen from various gap sizes was undertaken and the results are shown in Fig. 10; the lines parallel to the horizontal represent the calculated delays for the reflections from the front slab, with the other lines being reflections from the back surfaces. It is clear that the calculated reflection times are in good agreement with the predicted ones. Gap sizes of 100 μm can clearly be seen [see Fig. 11(a)], with the reconstruction showing good resolution of the first three reflections: the fourth reflection is not as clear, since the experimental signal is cut off shortly after it. Thus this reflection does not come out as clearly in the reconstruction. Gaps smaller than 100 μm are still partially resolved. Figure 11(b) shows reflections from the slabs with a 40 μm gap, but now the finite experimental pulse width causes a "smearing out" of the pulses reflected from either side of the gap, leading to an increase in the time between the two resolved pulses. This smearing out does not affect the pulse reflected from either the front surface of the first slab or back surface of the second slab.

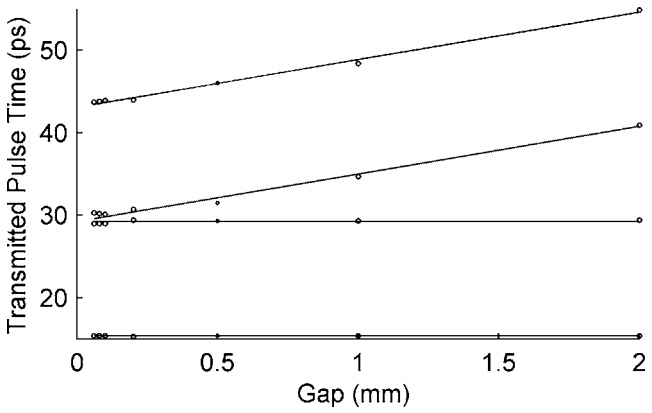

FIG. 10. Delay vs gap for PTFE slabs (reflection).

VI. CONCLUSION

We have developed postdetection signal processing software which, when applied to pulsed terahertz signals, will suppress the effects of echo signals and artifacts arising from the detection or generation devices or which are the results of atmospheric water absorption. In effect, the processing method delivers the impulse response of the device or sample under test and cleans up signals so that small, but genuine, effects caused by the interaction of the terahertz pulse with the sample can be observed. The method is validated by experimental transmission and reflection studies of simple phantom structures which mimic the behavior of a void or impurity located within another object.

It is concluded that the application of signal processing methods can significantly increase the ability of broadband terahertz techniques to image, for example, the internal structure of various samples, which might include laminated composites or contraband concealed within sealed documents. Experiments in transmission and reflection geometries with suitable phantoms show that significant signal to noise improvements are possible and that signals less than 2% in amplitude of the main pulse can be easily measured. Using the method, a resolution of less than 500 μm in transmission and 100 μm in reflection is readily obtainable. A higher resolution is seen in reflection measurements since these only require one interface reflection, as opposed to the two in transmission measurements. Thus, the reflected peak amplitudes in transmission are much lower than in reflection, so

merge more quickly into the background when they begin to overlap. One specific, and useful, conclusion of the work is that purging of terahertz TDS systems, to reduce atmospheric water absorption, may not be necessary if signal processing methods are used. A more general conclusion is that much more information, which is currently hidden, could be obtained if further attention were paid to terahertz signal processing methods.

ACKNOWLEDGMENTS

The authors wish to acknowledge the financial support of the following agencies and organizations: The Commission of the European Communities for the Integrated Project TeraNova (IST-511415) at Durham and Leeds, Her Majesty's Government Communications Centre (support of GPS at Durham), Research Councils UK for the award of a Basic Technologies Initiative grant at Leeds, and the North East Development Agency in the UK for general laboratory support at Durham.

[1] E. Pickwell and V. P. Wallace, J. Phys. D **39**, R301 (2006).
[2] G. Zhao, R. N. Schouten, N. Van der Valk, W. Th. Wenkebach, and P. C. M. Planken, Rev. Sci. Instrum. **73**, 1715 (2002).
[3] A. V. Oppenheimer and R. W. Shafer, *Discrete Time Signal Processing* (Prentice-Hall, Englewood Cliffs, NJ, 1998), pp. 477 and 448.
[4] Patent No. GB0708491.6 .
[5] J. R. Fletcher, G. P. Swift, DeChang Dai, J. M. Levitt, and J. M. Chamberlain, J. Appl. Phys. **101**, 013102 (2007).
[6] A. Burnett, W. Fan, P. C. Upadhya, J. Cunningham, E. H. Linfield, A. G. Davies, H. Edwards, T. Munshi, and A. O'Neil, Proc. SPIE **6120**, 155 (2006).
[7] Y. C. Shen, P. C. Upadhya, E. H. Linfield, H. E. Beere, and A. G. Davies, Appl. Phys. Lett. **83**, 3117 (2003).
[8] S. Kono, T. Tani, P. Gu, and K. Saka, Appl. Phys. Lett. **77**, 4104 (2000).